Subnetworks mediating feedforward and feedback processes revealed by multi-area Neuropixels recordings

Xiaoxuan Jia (xiaoxuanj@alleninstitute.org), Joshua H. Siegle (joshs@alleninstitute.org), Yazan N. Billeh (yazanb@alleninstitute.org), Séverine Durand (severined@alleninstitute.org), Greggory Heller (greggh@alleninstitute.org), Tamina Ramirez (taminar@alleninstitute.org), Anton Arkhipov (antona@alleninstitute.org), Shawn R. Olsen (shawno@alleninstitute.org)
Allen Institute for Brain Science
615 Westlake Ave N, Seattle, WA 98109

Abstract:

The visual system is organized hierarchically with feedforward and feedback pathways mediating cross-area communication. However, it is challenging to segregate these connections functionally and thus the logic of information flow remains unclear. Here, we studied this question by simultaneously recording from six visual cortical areas in awake mice with Neuropixels probes. We found two distinct neural ensembles based on their functional connectivity pattern: one ensemble is dominated by connections that drive the activity in the network ('driver'), while another ensemble is more driven by network activity ('driven'). 'Driver' neurons were more numerous in supragranular layers, whereas 'driven' neurons were more abundant in infragranular layers. Interestingly, although both 'driver' and 'driven' neurons were found across all cortical areas, the proportion of driven-to-driver cells systematically increased across the visual hierarchy. Strong directional information flow between these subnetworks was present during sensory stimulation, but not during spontaneous activity. The 'driver' ensemble showed earlier and more transient responses compared to the 'driven' ensemble. A rate model of the network recapitulated the link between response latency and functional connectivity. Overall, our study revealed distinct multi-area ensembles with distinct roles in information flow.

Keywords: visual cortex; functional connectivity; Neuropixels

Introduction

The mammalian visual cortex is organized hierarchically (Felleman & Van Essen, 1991; Markov et al., 2014), with increasing response latencies and enlarging receptive fields along the visual hierarchy (Freeman & Simoncelli, 2011; Lamme & Roelfsema, 2000). Information between different areas is transmitted through extensive axonal projections. A projection is considered feedforward when ascending from lower to higher areas of the hierarchy, but otherwise is feedback. It is generally assumed that the feedforward pathways propagate sensory information into the system, whereas the feedback pathways carry top-down signals such as prediction, expectation or attention to modulate or gate the sensory inputs (Gilbert & Li, 2013; Lamme, Supèr, & Spekreijse, 1998). However, since the cortical network is densely interconnected with feedforward, feedback, and horizontal connections, the logic of information transfer remains poorly understood.

Previous anatomical studies suggested that feedforward and feedback connections are cortical layer dependent. In primates, feedforward connections tend to originate in supragranular layers of the source area and target granular layers, whereas feedback projections tend to originate in infragranular layers and avoid targeting granular layers (Felleman & Van Essen, 1991; Markov et al., 2014). The fraction of projecting neurons in the supragranular layers of a source area reflect the hierarchical position (Barone, Batardiere, Knoblauch, & Kennedy, 2000; Markov et al., 2014). However, this general guideline is not absolute. For example, about half of the neurons that make feedback projections from V2 to V1 are located in the supragranular layers (Barone et al., 2000). Moreover, the organization of feedforward and feedback connections could be different across species (e.g. mice: Harris et al., 2018). Another complexity is that single cells can project to multiple target areas (Han et al., 2018). Thus, it is currently unclear how cross-area projections are utilized in feedforward and feedback processing in the mouse cortex.

Here we asked whether we could identify distinct neural ensembles in mouse visual cortex based on their patterns of functional connectivity derived from brief-timescale correlations in spiking activity between pairs of neurons. We sought to determine the spatial distribution of these neurons and address the roles of these different neural subnetworks in feedforward and feedback pathways based on their connectivity patterns, source and target layers, direction of functional influence relative to the visual hierarchy, and response dynamics.

Methods

Recording Setup and Experimental Design We developed a standardized platform to simultaneously

record from 6 Neuropixels probes (Jun et al., 2017) (Fig 1A, 384 densely arranged recording sites along a linear shank), which were inserted in mouse primary visual cortex (V1) and 5 higher-order visual cortical areas (LM, RL, AL, PM, and AM). During recording, mice were head-fixed but free to run on a wheel while viewing visual stimuli presented on a LCD monitor (Fig 1B). To maximize measurable functional connectivity across areas, we targeted regions with overlapping receptive fields (RF) guided by a retinotopic map (Fig 1C). Targeting was validated by mapping RFs of all cells with small Gabor patches presented at different locations on the screen. All analysis was restricted to neurons with well-defined receptive fields within the screen boundaries. To compare functional networks during distinct sensory input, we used three types of visual stimuli: drifting gratings, natural movies and mean luminance gray screen. On average, each recording session yielded 608±29 neurons (n = 16 mice; mean±SEM) simultaneously recorded from the 6 visual cortical areas.

Analysis Methods After spike sorting with *Kilosort* (Pachitariu et al., 2016), we analyzed functional interactions between simultaneously recorded neurons using jitter-corrected cross-correlograms (CCG) (Jia, Tanabe, & Kohn, 2013; Smith & Kohn, 2008). The jitter-corrected CCG reflects temporal correlations between a pair of neurons within the jitter-window (25ms). We derived the directed connection weight by subtracting the sum of (-13 to 0) ms of the CCG from the sum of (0 to 13) ms of the CCG. Computing this for each pair of neurons produced a directional connectivity matrix for each mouse (Fig. 2 A, B). In order to find neurons with shared connectivity pattern to the rest of the network, we clustered the directional connectivity matrix by treating the connectivity pattern from each source neuron to all target neurons as features. To remove redundancy, we projected the connectivity features into a lower dimensional space with principle component analysis (PCA). We applied a consensus clustering method to obtain robust clusters that are not biased by random initial conditions. First, we constructed a co-clustering probability matrix by running k-means with different initial conditions until the matrix is stable. Then, the probability matrix was clustered with hierarchical clustering. The number of clusters was determined by the elbow method.

Results

We found three clusters of neurons based on their shared connectivity patterns (Fig 2C): neurons in cluster 1 had mostly weak connections; cluster 2 neurons contained more positive connections that drive activity in the network; neurons in cluster 3 contained

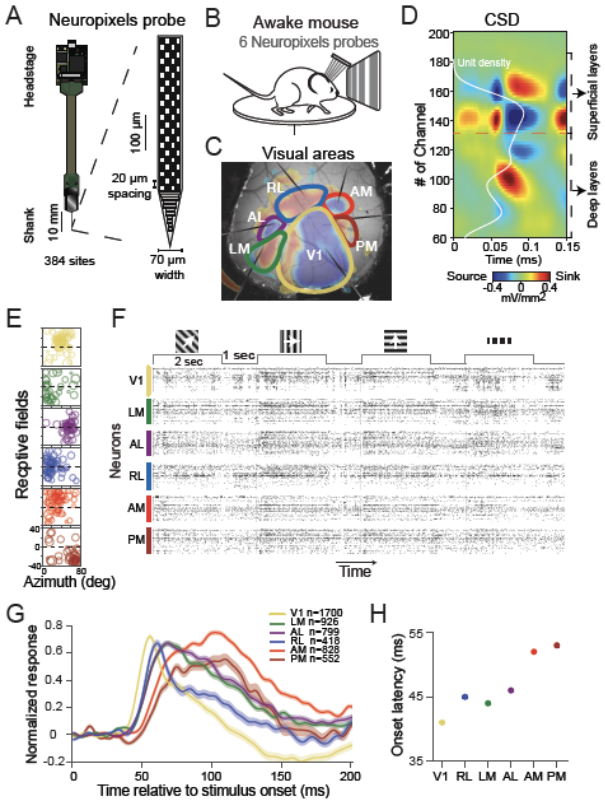

Figure 1. Multi-area Neuropixels recordings. A) Neuropixels probe. B) Recording setup. C) Visual cortical areas defined by retinotopic mapping. Colored outlines highlight the 6 visual areas. D) Current source density for layer estimation. E) RFs of units from an example mouse. Each circle represents the RF of one unit. F) Raster of simultaneously recorded cortical neurons (12 seconds with drifting grating stimuli). G) Normalized PSTH showing temporal response to drifting gratings (n=16 mice; legend show number units). H) Time to response onset (mean±SEM)

more negative connections. Based on the bias in the proportion of positive and negative connections from each cluster, we named cluster 2 neurons as the 'driver' ensemble and cluster 3 as the 'driven' ensemble. Interestingly, both 'driver' and 'driven' ensembles were distributed within and across cortical areas, but the relative proportion of these two clusters showed strong layer and area biases. The 'driver' neurons resided more in the supragranular layers, while the 'driven' neurons resided more in the infragranular layers (Fig 2E). The proportion of 'driver' vs 'driven' neurons systematically changed across the visual hierarchy (inferred from response latency (Fig 1H)), such that the fraction of driver neurons decreased along the hierarchy but driven neurons increased (Fig 2F). Consistent with these clusters representing functionally

distinct sets of neurons, the temporal dynamics of the 'driver' and 'driven' ensemble were significantly different. Neurons in the 'driver' ensemble showed earlier responses (mean time to peak=75±1.3ms) compared to those in the 'driven' ensemble (mean time to peak=90±1.0ms) (Fig 3).

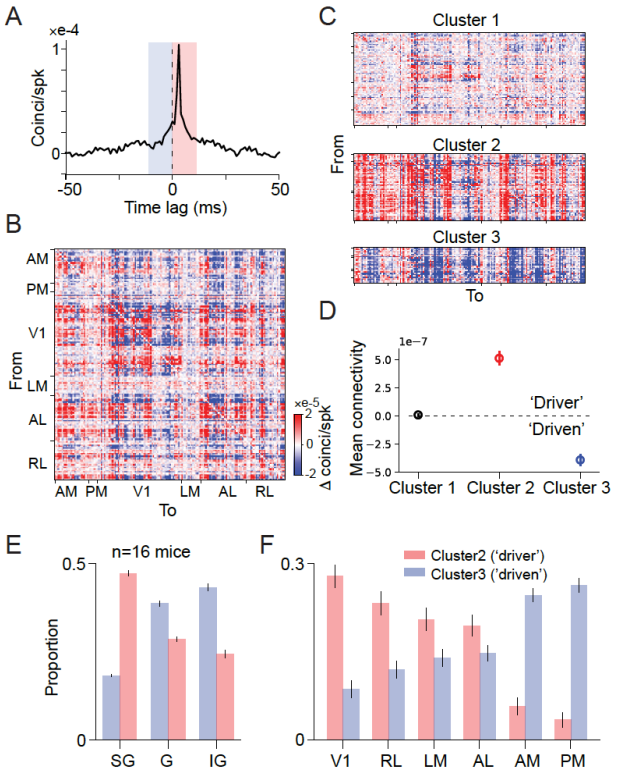

Figure 2. Distinct inter-area subnetworks defined by shared functional connectivity patterns. A) Example CCG. B) Directed connectivity matrix from an example mouse. Each matrix entry value represents the strength and directionality of the functional connectivity of one pair of neurons. C) Clustering on the directional connectivity matrix revealed 3 clusters. D) Averaged connection strength from each cluster to each neuron in the network (error bars represent 95% CI; n_cluster1=926; n_cluster2=846, n_cluster3=846 in 16 mice). E) Laminar distribution of the 'driver' and 'driven' neural ensembles. F) Proportion of 'driver' and 'driven' ensembles for different cortical areas.

Because distinct classes of visual stimuli drive the visual system differently, the neuronal response and functional interactions between neurons may change with stimuli. For example, drifting grating stimuli normally induce a strong coherent drive to the visual system, while natural movie stimuli with a different spatiotemporal structure normally induce sparser response patterns. Therefore, we compared the subnetworks from 'driver' to 'driven' ensembles across different stimuli, and found that drifting grating stimuli induced a strong information flow from the 'driver' ensemble to the 'driven' ensemble and natural movie stimuli induced a weaker but similar connectivity pattern. However, spontaneous activity (gray screen) showed little directional bias between the two ensembles. These results suggest that only when the network is driven by external stimuli is there a clear direction of information flow from the 'driver' to 'driven' neurons.

To explore the link between temporal dynamics and information flow between areas, we built a fully-connected, multi-area rate model based on the functional adjacency matrix measured in vivo. We generated the aggregated adjacency weight matrix by taking the mean amplitude of the sharp-peaks of putative monosynaptic CCGs between pairs of areas, separately for the 'driver' subnetwork and 'driven' subnetwork. Our model recapitulated the measured latency difference between the two neural ensembles within and across areas. This shows the network connectivity patterns are sufficient to produce the temporal dynamics suggesting a fundamental link between them.

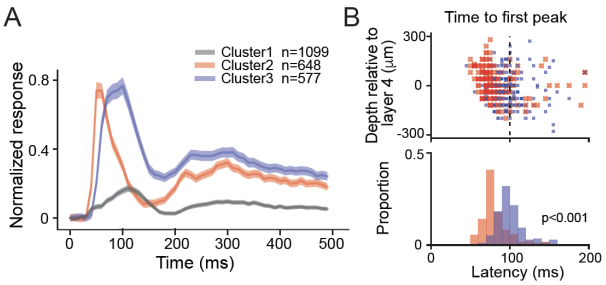

Figure 3. Distinct temporal dynamics in functional networks. A) Population average of normalized PSTH for different clusters. B) Layer dependency of time to peak in different neuronal ensembles. Top: Summary of time-to-peak at different depths relative to layer 4 (n=16 mice). Bottom: distribution of time to peak in different ensembles (Student t-test p = 2.8E-6 for time-to-peak between cluster 2 and 3).

Discussion

We identified two distinct cortical ensembles based on their functional connectivity patterns within the multi-area networks of mouse visual cortex. The 'driver' ensemble distribution is biased towards supragranular layers, whereas the 'driven' neurons were more prominent in infragranular layers. Importantly, the distribution of 'driver' vs 'driven' neurons systematically

changed across the visual hierarchy (defined in Harris et al., (2018)). Previous studies suggest that neurons mediating feedforward projections tend to originate in supragranular layers of the source area (Felleman & Van Essen, 1991; Markov et al., 2014), and the fraction of projecting neurons in supragranular layers decrease along the hierarchy (Barone et al., 2000). Because 'driver' neurons were biased for supragranular layers and their proportion in each area reduced along the visual hierarchy, it is likely that the 'driver' ensemble in each area is more involved in feedforward processing.

Our findings on cross-area functional connectivity suggest that distinct ensembles of neurons in each cortical area predominately either receive or provide long-range connections to other cortical areas. Moreover, our results indicate that 'driver' neurons functionally drive activity in multiple cortical areas; similarly, 'driven' neurons receive functional inputs from multiple sources. This distributed functional architecture could allow efficient, parallel processing across areas of the cortex. Lastly, unlike anatomical connectivity, the functional connectivity is a dynamic entity that can be restructured by external stimulus input.

Our results also suggested a link between neuronal dynamics and information flow. Neurons that responded earlier and more transiently sent information out of an area, whereas neurons that responded later with more sustained activity received input from other areas. This link is validated with a fully-connected rate model based on measured connectivity strength, indicating a fundamental relationship between network functional connectivity and temporal dynamics in response to external stimuli.

To our knowledge, this study is the first to measure single neuron-level functional connectivity with high temporal resolution in the multi-area cortical networks of the mouse visual system. Our analysis separated cortical neurons into distinct ensembles based on their functional connectivity to the network. The dynamics, layer, and hierarchical dependency suggest these functional-connectivity defined neuronal ensembles may participate differently in feedforward and feedback pathways, and thus provide a path to deciphering the information flow in the cortical network.

Acknowledgments

The work was supported by the Allen Institute. We thank Daniel J. Denman for helpful discussions.

References

Barone, P., Batardiere, A., Knoblauch, K., & Kennedy, H. (2000). Laminar distribution of neurons in extrastriate areas projecting to visual areas V1 and V4 correlates with the hierarchical rank and indicates the operation of a distance rule. *The Journal of Neuroscience, 20*(9), 3263–3281.

Felleman, D. J., & Van Essen, D. C. (1991). Distributed Hierarchical Processing in the Primate Cerebral Cortex. *Cerebral Cortex*, *1*(1), 1–47.

Freeman, J., & Simoncelli, E. P. (2011). Metamers of the ventral stream. *Nature Neuroscience*, *14*(9), 1195–1204.

Gilbert, C. D., & Li, W. (2013). Top-down influences on visual processing. *Nature Reviews Neuroscience*, *14*(5), 350–363.

Han, Y., Kebschull, J. M., Campbell, R. A. A., Cowan, D., Imhof, F., Zador, A. M., & Mrsic-Flogel, T. D. (2018). The logic of single-cell projections from visual cortex. *Nature*, *556*(7699), 51–56.

Harris, J. A., Mihalas, S., Hirokawa, K. E., Whitesell, J. D., Knox, J., Bernard, A., … Zeng, H. (2018). The organization of intracortical connections by layer and cell class in the mouse brain. *BioRxiv*, 292961.

Jia, X., Tanabe, S., & Kohn, A. (2013). γ and the coordination of spiking activity in early visual cortex. *Neuron*, *77*(4), 762–774.

Jun, J. J., Steinmetz, N. A., Siegle, J. H., Denman, D. J., Bauza, M., Barbarits, B., … Harris, T. D. (2017). Fully integrated silicon probes for high-density recording of neural activity. *Nature*, *551*(7679), 232–236.

Lamme, V. A., & Roelfsema, P. R. (2000). The distinct modes of vision offered by feedforward and recurrent processing. *Trends in Neurosciences*, *23*(11), 571–579.

Lamme, V. A., Supèr, H., & Spekreijse, H. (1998). Feedforward, horizontal, and feedback processing in the visual cortex. *Current Opinion in Neurobiology*, *8*(4), 529–535.

Markov, N. T., Ercsey-Ravasz, M. M., Ribeiro Gomes, A. R., Lamy, C., Magrou, L., Vezoli, J., … Kennedy, H. (2014). A Weighted and Directed Interareal Connectivity Matrix for Macaque Cerebral Cortex. *Cerebral Cortex*, *24*(1), 17–36.

Pachitariu, M., Steinmetz, N., Kadir, S., Carandini, M., & Harris K. D., (2016). Kilosort: realtime spike-sorting for extracellular electrophysiology with hundreds of channels. *BioRxiv*, 061481.

Smith, M. A., & Kohn, A. (2008). Spatial and Temporal Scales of Neuronal Correlation in Primary Visual Cortex. *J. Neurosci.*, (28), 12591–12603.